Bioorganic & Medicinal Chemistry 17 (2009) 401–410

Contents lists available at ScienceDirect

Bioorganic & Medicinal Chemistry

journal homepage: www.elsevier.com/locate/bmc

Novel potent and highly selective human A_3 adenosine receptor antagonists belonging to the 4-amido-2-arylpyrazolo[3,4-*c*]quinoline series: Molecular docking analysis and pharmacological studies

Vittoria Colotta [a,*], Francesca Capelli [a], Ombretta Lenzi [a], Daniela Catarzi [a], Flavia Varano [a], Daniela Poli [a], Fabrizio Vincenzi [b], Katia Varani [b], Pier Andrea Borea [b], Diego Dal Ben [c], Rosaria Volpini [c], Gloria Cristalli [c], Guido Filacchioni [a]

[a] *Dipartimento di Scienze Farmaceutiche, Laboratorio di Progettazione, Sintesi e Studio di Eterocicli Biologicamente Attivi, Università di Firenze, Polo Scientifico, Via Ugo Schiff, 6, 50019 Sesto Fiorentino, FI, Italy*

[b] *Dipartimento di Medicina Clinica e Sperimentale, Sezione di Farmacologia, Università di Ferrara, via Fossato di Mortara 17-19, 44100 Ferrara, Italy*

[c] *Dipartimento di Scienze Chimiche, Università di Camerino, via S. Agostino 1, 62032 Camerino, Italy*

ARTICLE INFO

Article history:
Received 29 July 2008
Revised 7 October 2008
Accepted 8 October 2008
Available online 11 October 2008

Keywords:
G protein-coupled receptors
Adenosine receptor antagonists
Pyrazoloquinolines
Tricyclic heteroaromatic systems
Ligand–receptor modeling studies

ABSTRACT

The study of novel 2-arylpyrazolo[3,4-*c*]quinolin-4-(hetero)arylamides, designed as human (h) A_3 adenosine receptor antagonists, is reported. The new derivatives are endowed with nanomolar hA_3 receptor affinity and high selectivity versus hA_1, hA_{2A} and hA_{2B} receptors. Among the (hetero)aroyl residues introduced on the 4-amino group, the 2-furyl and 4-pyridyl rings turned out to be the most beneficial for hA_3 affinity (K_i = 3.4 and 5.0 nM, respectively). An intensive molecular docking study to a rhodopsin-based homology model of the hA_3 receptor was carried out to obtain a 'structure-based pharmacophore model' that proved to be helpful for the interpretation of the observed affinities of the new hA_3 pyrazoloquinoline antagonists.

1. Introduction

Adenosine is a neuromodulator which exerts a host of physiopathological effects through activation of four receptor subtypes, belonging to the superfamily of G protein-coupled receptors and termed A_1, A_{2A} A_{2b} and A_3 adenosine receptors (ARs).[1,2] The A_3 receptor subtype has a widespread distribution, both in the brain and peripheral systems,[1,2] and couples to different second messenger pathways such as inhibition of adenylyl cyclase,[2] stimulation of phospholipase C[3] and D[4] and activation of K_{ATP}channels.[5] A_3 AR, like the other ARs, also couples to members of the mitogen-activated protein kinase (MAPK) family, such as the extracellular signal-regulated kinase (ERK)1/2 and p38,[6] and this coupling gives this receptor a role in cell growth, survival, death and differentiation.[6,7] Interestingly, A_3 AR activation may afford both cell protection and cell death, being strictly dependent on the degree of receptor activation and/or the cell type.[7,8] For A_3 AR antagonists different potential therapeutic applications have been envisaged. They could be useful tools for the treatment of glioblastoma multiforme,[9] as renal protective drugs[10] and in the treatment of glaucoma.[11] Recently, they have also been investigated as neuroprotective agents.[12–14] In our laboratory, much effort has been directed toward the study of hA_3 AR antagonists belonging to different classes of heteroaromatic derivatives,[14–20] and one of the most recently investigated is represented by the 4-amido-2-arylpyrazolo[3,4-*c*]quinoline series[14,16] (Chart 1). Structure–activity relationship studies showed that the presence of acyl substituents on the 4-amino group positively affects both A_3 AR affinity and selectivity, one of the most advantageous residues being a benzoyl moiety (Chart 1, compound **1**). Introduction of small groups (R = 3- or 4-Me, 3- or 4-OMe) on the 2-phenyl ring of the 4-amido derivatives, although it maintained the hA_3 affinity in the nanomolar range, reduced the selectivity toward this receptor. On the basis of these findings, and taking **1** as lead compound, we synthesized the new derivatives **2–23** (Chart 1), most of which lack substituents on the 2-phenyl ring (**2–13, 18–23**) while bearing various heteroaroyl (**2–15**) or aroyl (**18–21**) moieties on the 4-amino group. We also prepared the 4-diaroylamino derivatives **22–23** because previous data showed that introduction of a second benzoyl residue on the 4-amino group of compound **1** maintained both high hA_3 affinity and selectivity.[14]

A molecular docking analysis of the new derivatives **2–23** and of the lead **1** was performed using a homology model of human A_3 receptor based on the bovine rhodopsin crystal structure as a

* Corresponding author. Tel.: +39 55 4573731; fax +39 55 4573780.
E-mail address: vittoria.colotta@unifi.it (V. Colotta).

0968-0896/$ - see front matter © 2008 Elsevier Ltd. All rights reserved.
doi:10.1016/j.bmc.2008.10.018

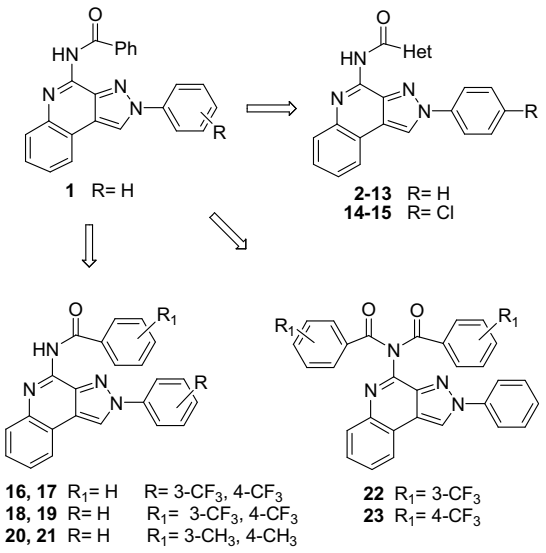

Chart 1. Previously and herein reported 2-arylpyrazolo[3,4-*c*]quinolin-4-amido derivatives.

template. Docking results were compared to biological data with the aim of defining the SAR profile of the compounds and obtaining useful information for the rational design of new hA_3 AR antagonists.

2. Chemistry

The target 4-amido derivatives **2–23** were obtained starting from the 2-arylpyrazolo[3,4-*c*]quinolin-4-amines **24**,[14,16] **25**,[16] **26** and **27** which were prepared following the pathway depicted in Scheme 1. Briefly, a mixture of 3-ethoxalylindole[21] with the suitable arylhydrazine hydrochloride in absolute ethanol and a few drops of glacial acetic acid was microwave irradiated at 140 °C for 3 min to afford the 2-arylpyrazolo[3,4-*c*]quinolin-4-ones **28**,[14,16] **29**,[16] **30** and **31**. Compounds **28–31**were reacted with a mixture of phosphorus pentachloride/phosphorus oxychloride to give the corresponding 4-chloro derivatives **32**,[14,16] **33**,[16] **34** and **35** which were transformed into the desired 4-amino derivatives **24–27** with ammonia. The target 2-arylpyrazoloquinolin-4-amides 2–**21**(Scheme 2) were obtained by reacting **24–27** with the suitable

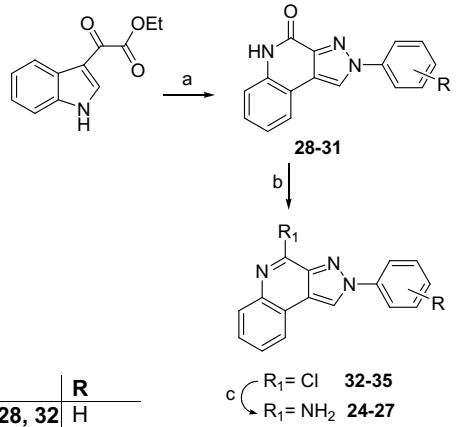

	R
24, 28, 32	H
25, 29, 33	4-Cl
26, 30, 34	3-CF_3
27, 31, 35	4-CF_3

Scheme 1. Reagents and conditions: (a) arylhydrazine hydrochloride, absolute EtOH, AcOH, microwave irradiation; (b) $PCl_5/POCl_3$; (c) NH_3(g), absolute EtOH.

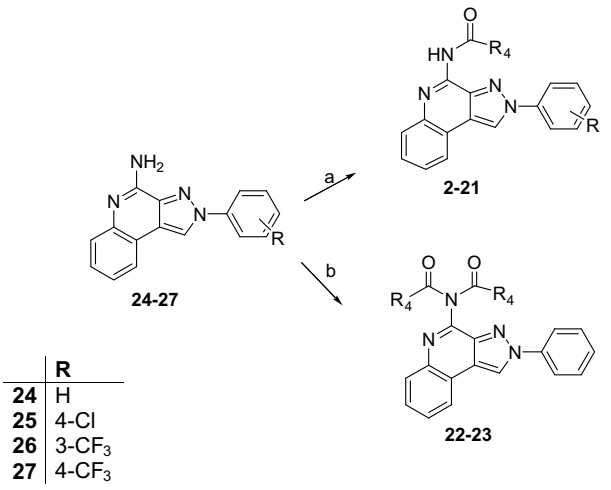

	R
24	H
25	4-Cl
26	3-CF_3
27	4-CF_3

	R_4	R		R_4	R
2	2-furyl	H	**13**	2-pyrazinyl	H
3	3-furyl	H	**14**	4-pyridyl	Cl
4	2-(5-methylfuryl)	H	**15**	2-furyl	Cl
5	2-thienyl	H	**16**	C_6H_5	3-CF_3
6	3-thienyl	H	**17**	C_6H_5	4-CF_3
7	4-thiazolyl	H	**18**	C_6H_4-3-CF_3	H
8	2-pyridyl	H	**19**	C_6H_4-4-CF_3	H
9	3-pyridyl	H	**20**	C_6H_4-3-CH_3	H
10	4-pyridyl	H	**21**	C_6H_4-4-CH_3	H
11	2-pyrimidyl	H	**22**	C_6H_4-3-CF_3	
12	4-pyrimidyl	H	**23**	C_6H_4-4-CF_3	

Scheme 2. Reagents: (a) Suitable carboxylic acid, 1-hydroxybenzotriazole, NEt_3, 4-(dimethylamino)pyridine, 1-(3-(dimethylamino)propyl)-3-ethylcarbodiimide hydrochloride, DMF; (b) ArCOCl, anhydrous pyridine, methylene chloride.

carboxylic acids in dimethylformamide and in the presence of 1-hydroxybenzotriazole, triethylamine, and 4-(dimethylamino)pyridine. Most of the used carboxylic acids were commercially available, except for 5-methylfuran-2-carboxylic acid,[22] 2-pyrimidyl-carboxylic acid[23] and 4-pyrimidyl-carboxylic acid,[24] which were synthesized following the reported procedures. Finally, the 4-diaroylamino derivatives **22** and **23** were obtained by refluxing the 4-amino derivative **24** with an excess of 3-trifluoromethylbenzoyl chloride and 4-trifluoromethylbenzoyl chloride, respectively, in anhydrous methylene chloride and pyridine.

3. Pharmacology

The 4-amido derivatives **2–23**, and their newly synthesized precursors, i.e., the 4-amino-2-arylpyrazoloquinolines **26**, **27** and the corresponding 4-oxo compounds **30** and **31** were tested for their ability to displace [^{3}H]8-cyclopentyl-1, 3-dipropylxanthine (DPCPX), [^{3}H]4-(2-[7-amino-2-(2-furyl)[1, 2, 4]triazolo[2, 3-*a*][1,3,5]triazin-5-yl-amino]ethyl)phenol (ZM 241385) and [^{125}I]N^6-(4-amino-3-iodobenzyl)-5′-(*N*-methylcarbamoyl) adenosine (AB-MECA), respectively, from cloned hA_1, hA_{2A} and hA_3 ARs stably expressed in CHO cells. Compounds **2–23**, **26**, **27**, **30**, **31** were also tested at the hA_{2B} subtype by measuring their inhibitory effects on NECA-stimulated cAMP levels in CHO cells stably transfected with the hA_2B AR. The antagonistic potencies of the selected derivatives **2**, **4**, **8–10**, **14**, **15**, **20** and **21** were assessed by evaluating their effect on 2-chloro-N^6-(3-iodobenzyl)-5′-(*N*-methylcarbamoyl) adenosine (Cl-IB-MECA)-inhibited cAMP production in CHO cells, stably expressing hA_3 ARs. Finally, compounds **2**, **4**, **8–10**, **14**, **15**, **20** and **21** were also tested to evaluate their affinities at the rat A_3 AR, stably expressed in HEK 293 cells. All pharmacological data are collected in

Table 1
Binding affinity at hA_1, hA_2A and hA_3 ARs and Potencies at hA_2B and hA_3

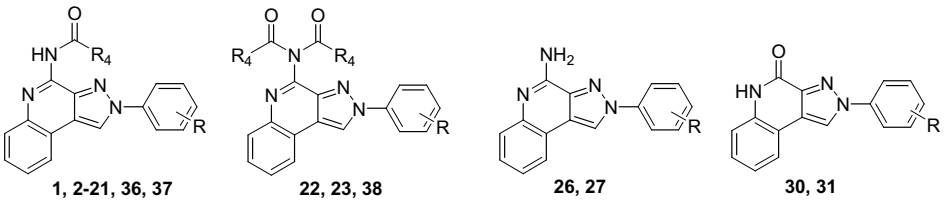

			Binding experiments K_i (nM) or I%				cAMP assays IC_{50} (nM) or I%	
	R_4	R	hA_3[a]	rA_3[b]	hA_1[c]	hA_2A[d]	hA_{2B}[e]	hA_3[f]
1[g]	C_6H_5	H	2 ± 0.1		0%	0%	Nt[h]	Nt[h]
2	2-Furyl	H	3.4 ± 0.3	29%	34%	20%	3%	21 ± 3
3	3-Furyl	H	50 ± 6		9%	2%	5%	
4	2-(5-Methylfuryl)	H	7.5 ± 0.8	30%	500 ± 53	10%	5%	49 ± 5
5	2-Thienyl	H	50 ± 6		45%	1%	6%	
6	3-Thienyl	H	40 ± 5		1%	2%	2%	
7	4-Tiazolyl	H	60 ± 5		12%	1%	2%	
8	2-Tyridyl	H	15.5 ± 1.3	23%	3%	9%	15%	107 ± 9
9	3-Pyridyl	H	10.5 ± 1.7	27%	26%	1%	1%	76 ± 5
10	4-Pyridyl	H	5.0 ± 0.6	26%	8%	1%	1%	41 ± 4
11	2-Pyrimidyl	H	945 ± 82		6%	2%	1%	
12	4-Pyrimidyl	H	210 ± 18		9%	6%	3%	
13	2-Pyrazinyl	H	65 ± 6		6%	6%	2%	
14	2-Furyl	4-Cl	11.5 ± 1.5	11%	17%	1%	2%	83 ± 7
15	4-Pyridyl	4-Cl	24.7 ± 2.9	21%	4%	2%	3%	145 ± 12
16	C_6H_5	3-CF_3	52 ± 5		13%	1%	3%	
17	C_6H_5	4-CF_3	140 ± 15		10%	1%	3%	
18	C_6H_4-3-CF_3	H	60 ± 8		23%	1%	2%	
19	C_6H_4-4-CF_3	H	415 ± 37		10%	3%	4%	
20	C_6H_4-3-CH_3	H	6.3 ± 0.7	5%	20%	1%	35%	26 ± 3
21	C_6H_4-4-CH_3	H	11.5 ± 1.2	7%	6%	1%	38%	54 ± 5
22	C_6H_4-3-CF_3	H	24%		4%	3%	6%	
23	C_6H_4-4-CF_3	H	6%		17%	1%	1%	
26	H	3-CF_3	17%		6%	7%	4%	
27	H	4-CF_3	11%		1%	1%	11%	
30		3-CF_3	4%		2%	5%	3%	
31		4-CF_3	480 ± 50		6%	10%	5%	
36[g]	C_6H_5	3-CH_3	4.3 ± 0.5		57 ± 4.2	2860 ± 224	Nt[h]	
37[g]	C_6H_5	4-CH_3	4.4 ± 0.2		629 ± 51	26%	Nt[h]	
38[g]	C_6H_5	H	6.1 ± 0.5		0%	0%	Nt[h]	

[a] Displacement of specific [^{125}I]AB-MECA binding to hA_3CHO cells. K_i values are means ± SEM of four separate assays each performed in duplicate.
[b] Percentage of inhibition in [^{125}I]AB-MECA competition binding assays to rA_3 HEK cells by using 1 μM concentration of the tested compounds.
[c] Percentage of inhibition in [^{3}H]DPCPX competition binding assays to hA_1CHO cells by using 1 μM concentration of the tested compounds; the K_i value is the mean ± SEM of four separate assays each performed in duplicate.
[d] Percentage of inhibition in [^{3}H]ZM241385 competition binding assays of the tested compounds (1 μM) to hA_{2A}CHO cells.
[e] Percentage of inhibition of the examined compounds at the 1 μM concentration on cAMP experiments in hA_{2B}CHO cells stimulated by 200 nM NEC A (NEC A EC_{50} = 150 ± 12 nM).
[f] IC_{50} values of the examined compounds (1 nM–l μM) are expressed as means ± SEM of four separate cAMP experiments in hA_3CHO cells which were inhibited by 100 nM Cl-IB-MECA (Cl-IB-MECAEC_{50} = 10 ± l nM).
[g] Ref. 14.
[h] Not tested.

Table 1, together with the binding results of the previously reported 2-arylpyrazoloquinolin-4-amides **1, 36–38**[14] included as reference antagonists.

4. Results and discussion

4.1. Structure–affinity relationships

The binding data, reported in Table 1, show that replacement of the benzoyl moiety of the lead compound 1 with various (hetero)aroyl rings generally maintains high hA_3 AR affinity. In fact, several of the new derivatives (compounds **2–6, 8–10, 14, 15, 20, 21**) show low K_i values (K_i < 50 nM). Interestingly, all the newly synthesized 4-amido derivatives **2–23** possess complete hA_3 selectivity, being totally unable to bind hA_1, hA_2 A and hA_2B receptors, with the only exception of compound **4** which shows some hA_1 affinity. As expected on the basis of previous data on 4-amidopirazolo[3,4-*c*]quinolines,[14] all derivatives tested at the rat A_3 receptor (compounds **2**, **4**, **8–10, 14, 15, 20** and **21**) do not show any appreciable affinity for this receptor.

Among the probed heterocyclic substituents, the 2-furyl and 2- or 3- or 4-pyridyl rings revealed to be the most beneficial, since compounds **2, 8–10** display the highest hA_3 affinity (K_i = 3.4–15 nM) Introduction of a 5-methyl group in the furyl moiety of derivative **2** afforded compound **4** which still possesses a high hA_3 binding activity (K_i = 7.5 nM). Replacement of the 2-furyl ring of **2** with other pentacyclic substituents, such as 3-furyl, 2- or 3-thienyl and 4-thiazolyl (compounds **3, 5–7**), causes some reduction of the hA_3 affinity (K_i = 50–60 nM). When a second nitrogen atom was introduced in the pyridyl moiety, a drop of hA_3 affinity was observed for the 2- and 4-pyrimidyl derivatives **11** and **12** (K_i = 945 and 210 nM, respectively), while for the 2-pyrazinyl derivative **13** a good hA_3 affinity (K_i = 65 nM) was obtained. As stated above, most of the newly synthesized derivatives lack the R substituent on the 2-phenyl group, since in a previous study[14] we found that the presence of R = Me or OMe, either in the *para*-

or *meta-position*, while maintaining a high hA_3 affinity, reduced the hA_3 versus hA_1 selectivity, as can be noted by comparing the binding data of compound **1** with those of the previously reported derivatives **36**[14] (R = 3-Me) and **37**[14] (R = 4-Me) (Table 1). Instead, the presence of R = 4-Cl (compounds **14** and **15**), although slightly reducing the hA_3 affinity, retains high hA_3 selectivity (compare compounds **2** and **10**–**14** and **15**, respectively).

The rationale for the synthesis of compounds **16–21** ensued from molecular modeling findings (see Section 4.2 for details). Introduction of the CF_3 substituent on the 2-phenyl ring, both in *meta*- (**16**) and *para*- (**17**) positions (K_i = 52 and 140 nM, respectively), reduced the hA_3 AR affinity, either compared to that of the lead compound 1 (R = H) or to those of compounds **36**[14](R = 3-Me) and **37**[14] (R = 4-Me). A reduction of hA_3 affinity was also obtained when the CF_3 group was introduced in the *meta*- (**18**) or *para*-position (**19**) of the benzoylamino moiety. Indeed, compounds **18** and especially **19** show lower hA_3 affinities (K_i = 60 and 415 nM, respectively) in comparison to the lead derivative **1** (K_i = 2 nM). In contrast, introduction of the Me substituent on the benzoylamino group of the lead **1**, both in *meta*- (**20**) and *para*- (**21**) positions, did not change much the hA_3 affinity (K_i = 6.3 nM and 11.5 nM, respectively) which remains in the low nanomolar range.

Derivatives **22** and **23**, bearing, respectively, a *meta*- and *para*-CF_3 group on the two benzoyl moieties, displayed null hA_3 AR affinities. These data, if compared to the high hA_3 AR affinity of the 4-dibenzoylamino derivative **38**[14] (Table 1), may be ascribed to the electron-withdrawing properties and steric hindrance of the CF_3 substituent, which might cause a change in electron density on the molecule and a distortion of the binding mode at the receptor.

The hA_3 affinity values of the 4-amino- and 4-oxo-substituted 2-arylpyrazoloquinolines **26, 27** and **30, 31**, synthetic precursors of the target derivatives **16** and **17**, were quite unexpected. Indeed, on the basis of the hA_3 nanomolar affinity of many previously reported 2-arylpyrazoloquinolin-4-ones and 4-amines,[14] also these new 2-aryl derivatives, bearing a 3-CF_3 (**26, 30**) or 4-CF_3 (**27, 31**) group on the 2-phenyl ring, were expected to possess at least some affinity for this receptor subtype. On the contrary, only the 4-oxo derivative **31** showed some capability to bind to the hA_3 AR, thus confirming that in this series of derivatives the CF_3 group on the 2-phenyl ring does not have a beneficial role.

Derivatives **2, 4**, **8–10, 14, 15, 20**, **21**, which showed the highest hA_3 AR affinities (K_i < 30 nM), were tested in cAMP assays to evaluate their potencies towards the hA_3 receptor. Consistently with their hA_3 affinity values, the tested compounds proved to be potent in inhibiting the NECA-inhibited cAMP accumulation in hA_3 CHO cells, thus showing an antagonistic behavior (Table 1).

4.2. Molecular modeling studies

A molecular docking analysis of the pyrazoloquinoline derivatives was performed on a homology model of hA_3 receptor based on the bovine rhodopsin crystal structure as template, with the aim of obtaining a possible rationalization of the different binding affinities for the hA_3 receptor.

As the preliminary model of hA_3 receptor did not contain a suitable cavity acting as binding site, this region was defined with the aid of published site directed mutagenesis data, which indicated, in particular, that the residues His95, Ser247, Asn250, and His272 are important for antagonist binding.[25] Thus, a manual docking section was performed on the lead compound **1** which was inserted in different orientations in the defined binding cavity. Consequently, an equivalent number of protein–ligand complexes were obtained. Each complex was then energetically minimized, and the potential energy of the different receptor conformations (extracted from the respective receptor–ligand complexes) was measured. The receptor conformation with the lowest potential energy value was selected for the docking section. For each ligand, docking studies allowed generation of a set of possible docking poses which were energetically minimized and re-scored.

The binding cavity is inserted between TM3 (Met86, Thr87, Leu90, Leu91, T94, His95), EL2 (Ser165, Gln167, Phe168, Met172), TM5 (Val178, Phe182, Ile186) TM6 (Trp243, Leu246, Ser247, Asn250, Tyr254) and TM7 (Ile268) and has a clear Y shape.

Docking results showed that each ligand is able to interact with the receptor binding cavity by assuming different orientations which can be grouped into three families (Fig. 1). In the first conformation family (family 'A'), the pyrazoloquinoline scaffold is positioned in a space between TM3, TM5 and TM6, while the substituents at the 2- and 4-positions are located between TM5 and TM6 and between TM3 and TM7, respectively. The second conformation family (family 'B') shows ligands oriented in a symmetric way with respect to family 'A'. In fact, the pyrazoloquinoline nucleus is still located in a space between TM3, TM5 and TM6, while the 2- and 4-substituents are positioned, respectively, between TM3 and TM7 and between TM5 and TM6. The third conformation family (family 'C') is different as the pyrazoloquinoline scaffold is located between TM5 and TM6, while the 2- and 4- substituents are positioned between TM3 and TM7 and between TM3, TM5 and TM6, respectively.

For each docking conformation family, we considered the highest conformation score obtained for each ligand with the two scoring panels implemented in MOE[26] (London dG and Affinity dG). In some cases, within the same conformation family, we found the same conformation as the 'best one' for the same ligand, with both scoring function panels. Hence, six sub-databases (two per family considering the two scoring functions) were obtained. The calculated scores were then correlated with experimental binding affinities (pK_i), and Affinity dG scores in particular were able to give a ranking reasonably in accordance with pK_i data, as can be viewed in Fig. 2. London dG scores were unsuccessful in the same task. Considering the average Affinity dG score for each conformation family, it can be noticed even that the 'B' conformations seem the favorite among the three families. On the other hand, R square

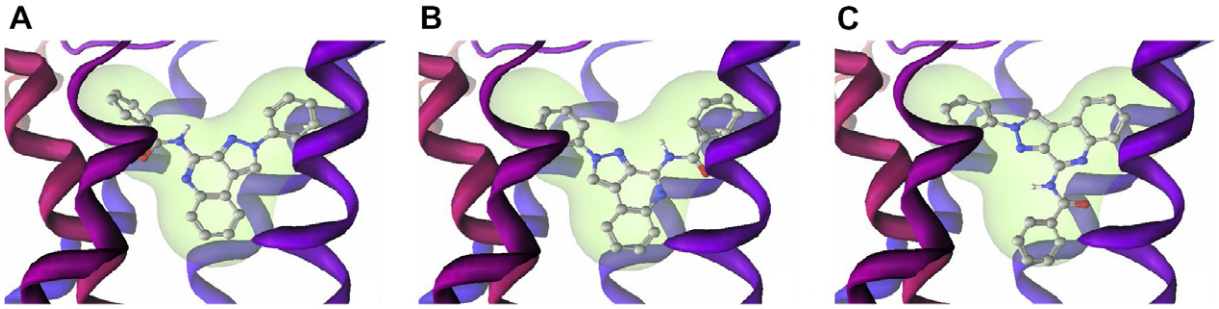

Figure 1. Left to right, in order A, B and C docking conformation families; the three docking conformations for compound **1** are shown.

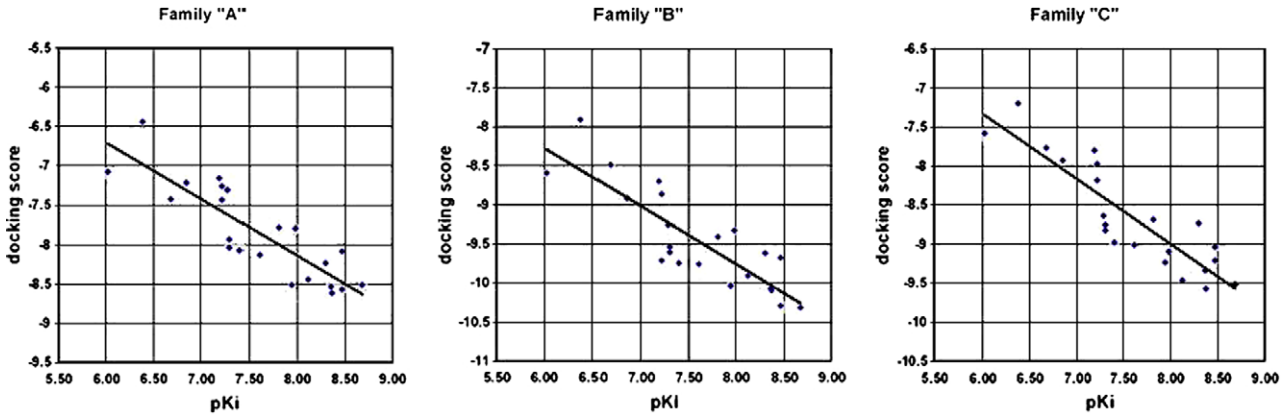

Figure 2. Left to right, experimental pK_i-docking score plots for the three conformation families. Docking scores in plots were calculated with MOE Affinity dG scoring function for minimized docking conformations (see Section 6 for details). Family A: average docking score = −7.85; correlation R^2 = 0.7412. Family B: average docking score = −9.45; correlation R^2 = 0.7187. Family C: average docking score = −8.66; correlation R^2 = 0.7568.

coefficients calculated for pK_i-score correlations indicate that family 'C' conformation ranking is more in accordance with p$K_i$data compared to the other families.

Interestingly, the three resulting docking conformation families show a similar binding motif, with the pyrazolo-pyridine portion of the scaffold located in correspondence with the 'Y-shaped' binding site core, and three aromatic rings (i.e., the fused benzo ring and the (hetero)aryl groups at the 2-position and on the 4-carbamoyl residue) positioned in the peripheral pockets. In addition, the 4-arylamido carbonyl group and the N5 atom are oriented toward Ser247 or Thr94, working as hydrogen bonding acceptors. Thus, a pharmacophore model can be obtained which consists of three 'peripheral' hydrophobic/aromatic features and two possible hydrogen bond acceptor features in proximity of Ser247 and Thr94. Depending on the docking conformation family, an aryl group is present in correspondence with each hydrophobic/aromatic feature, while at least one of the two H-bond acceptor features is matched by the carbonyl group in the 4-arylamido substituent and the N5 atom. Thus, at least four out of five features of the derived pharmacophore model are matched by each docking conformation family (Fig. 3).

These findings are consistent with previous docking studies,[14,25,27,28] in particular with those we achieved on previously synthesized 4-amidopyrazoloquinoline derivatives.[14] In this previous work, the docking conformation proposed for compound **1** (namely compound **17** in Ref. 14) belongs to the 'C' docking conformation family.

In addition, Tafi and co-workers published a pharmacophore-based modeling study in which pharmacophore hypotheses were used as guide points to build and refine a hA_3 receptor model for a subsequent docking study.[27] In another work, Moro and colleagues used a combined structure-based and ligand-based drug design strategy to identify common key structural features of pyrazolo-triazolo-pyrimidine derivatives as hA_3 antagonists.[28]

Very interestingly, our pharmacophore model presents similarities with regard to the types and 3D organizations of features suggested in both Tafi's and Moro's works.

The pharmacophore map is important to describe the general interaction scheme of the hA_3 pyrazoloquinoline antagonists with the receptor. However, the nature of the substituent either at the 4-carbamoyl group or on 2-phenyl ring is critical to differentiate potent from weak compounds. The benzoyl group of the lead compound **1** can be replaced by diverse heteroaroyl residues, such as the 2-furoyl and 2-(5-methylfuroyl) moieties (compounds **2** and **4**), and the 2- or 3- or 4-pyridoyl groups (derivatives **8**–**10**), which afford high hA_3 AR affinity (K_i < 15 nM). Instead, R_4 = 2- and 3-thienyl,

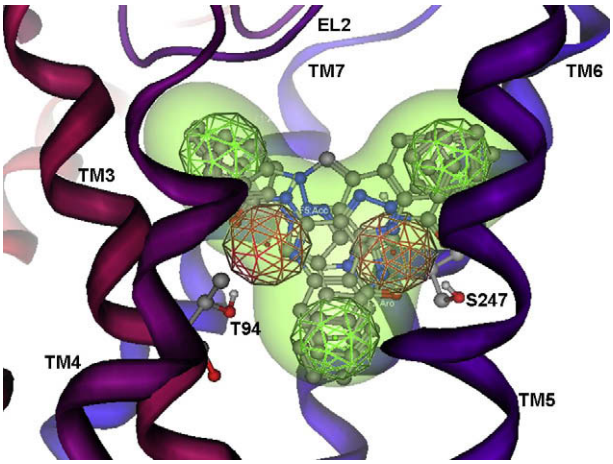

Figure 3. Superimposition of the three docking conformations of compound 1 (one conf. per family) and depiction of 3D pharmacophore. Three hydrophobic/aromatic features (green color) are located at peripheral points of Y-shaped binding site, while two H-bond acceptor features represent the two possible locations of the acceptors couple (the 4-arylamido carbonyl group substituent and the N5 atom) in proximity of Thr94 or Ser247 residues.

4-thiazolyl and 2-pyrazinyl rings (compounds **5–7**, **10**)caused some reduction of hA_3 AR affinity (K_i = 50–65 nM) which was much more marked in the case of the 2-and 4-pyrimidyl groups (**11** and **12**, K_i = 945 and 210 nM). These results can be rationalized if we consider that, in the Y-shaped binding site, the three peripheral anchoring areas are basically hydrophobic, even if a particular balance of hydrophobicity, aromaticity, and polarizability is required. In this sense, introduction of electron-rich heterocycles would not improve interaction with the hA_3 receptor, and the same applies to aromatic rings substituted with strong electron-withdrawing groups.

In order to confirm that this series of antagonists might assume at least two different orientations within the hA_3 receptor binding site (Fig. 4B and C) and to validate the proposed pharmacophore model, compounds **16–21, 36** and **37**, bearing a CF_3 or Me group on the 2-phenyl moiety or on the 4-aroylamino group, were investigated. The binding data indicate that introduction of a *meta*- or *para*-*Me* substituent in the 2-phenyl ring (**36**, **37**) or in the benzoyl pendant (**20**, **21**) of the lead compound **1** exerted the same effect. Indeed, compounds **36**[14] and **37**[14] possess the same hA_3 affinity of the new derivatives **20** and **21**. Quite similar results have been found for derivatives bearing the 3-CF_3 (**16** and **18**) and the 4-CF_3 substituent (**17** and **19**): derivatives **16** (K_i = 52 nM) and **18** (K_i = 60 nM) possess

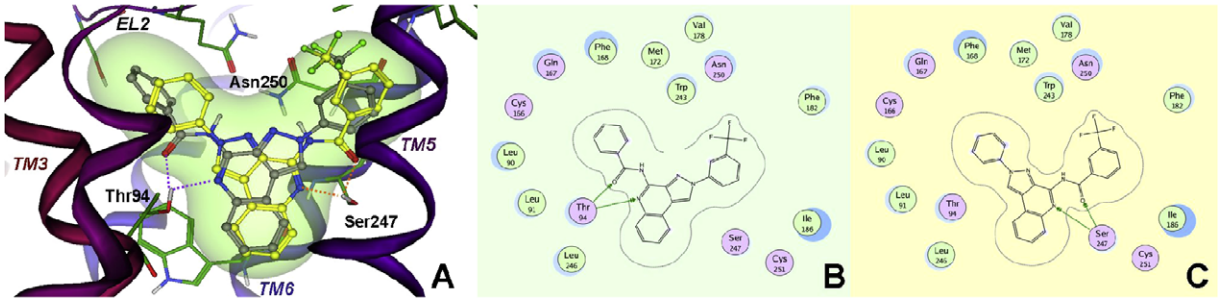

Figure 4. (A) Superimposition of 'A' docking conformation of compound 16 (hA_3 K_i = 52 ± 5 nM) and 'B' docking conformation of compound **18** (hA_3 K_i = 60 ± 8 nM); **18** is colored in yellow; H-bond interactions of **16** with hA_3 (Thr94 residue) are in lilac dash lines, while H-bond interactions of **18** with hA_3 (Ser247 residue) are in orange dash lines. (B) Schematic view of **16** 'A' docking conformation within hA_3 binding site; H-bond interactions with Thr94 residue are indicated. (C) Schematic view of **18** 'Bss' docking conformation within hA_3 binding site; H-bond interactions with Ser247 residue are indicated.

the same hA_3 affinity, while for compounds **17** and **19** only a three-fold difference exists between their hA_3 affinities (**17**: K_i = 140 nM; **19**: K_i = 415 nM). These findings confirm that the 4-amido-2-arylpyrazolo[3,4-*c*]quinoline derivatives can bind to the hA_3 receptor with at least two possible binding modes, belonging to the two conformation families 'A' and 'B', in which the 2-aryl or the 4-(hetero)aroylamino moiety occupy the same lipophilic pocket.

The significantly lower hA_3 AR affinities of the CF_3-substituted compounds **16–20**, with respect to those of the corresponding CH_3-substituted derivatives **20**, **21**, **36** and **37**, could be ascribed to the strong electron-withdrawing properties of the trifluoromethyl group which might cause a change in electron density on the molecule and a distortion of the binding mode at the receptor. Also the higher steric hindrance of the trifluoromethyl group, with respect to that of the methyl substituent, might have a role in reducing the anchoring to the receptor site.

Molecular modeling tools were also used for a further analysis in order to estimate the druggability of the reported pyrazoloquinoline derivatives. In this sense, a set of molecular descriptors (log*P*, log*S*, molecular weight, number of H-bond donors and acceptors, water accessible surface area) were calculated and analyzed in comparison with Lipinski's 'rule-of-five' filter (log*P* < 5; molecular weight < 500; number of H-bond donors < 5; number of H-bond acceptors < 10) (see Section 6.2.6 for further details). Among these calculated descriptors, log*P* and log*S* represent, respectively, the log of the octanol/water partition coefficient and the log of the aqueous solubility (mol/L); the water accessible surface area parameters (water accessible surface area, ASA; hydrophobic surface area, ASA_H; polar surface area, ASA_P) were also calculated as related to the ability of molecules to get solvated.

The results of this analysis show that, on the whole, the reported compounds present a good 'druggability' profile, and some of them (**1–13, 15, 26–31**) do not violate any Lipinski parameter. In addition, ASA_H, log*S* and log*P* values are well correlated, and the estimated log*S* and log*P* values indicate a reasonable solubility for several of these compounds (many of them presenting a log*P* value < 4).

5. Conclusion

This study describes a new set of 4-(hetero)aroylamino-2-arylpyrazolo[3,4-*c*]quinoline derivatives as potent and highly selective hA_3 receptors antagonists. Molecular modeling studies showed the ability of this class of compounds to assume different orientations within the hA_3 receptor homology model binding site, even maintaining the interaction scheme with receptor residues. Docking results showed an interesting correlation between docking scores and experimental binding data, and they were employed to develop a pharmacophore model which could be helpful for the interpretation of the observed affinities and for the design of new hA_3 pyrazoloquinoline antagonists. Several of the new derivatives showed a good druggability profile as they adhere to Lipinski's 'rule-of-five'.

6. Experimental

6.1. Chemistry

Microwave-assisted syntheses were performed using an Initiator EXP Microwave Biotage instrument (frequency of irradiation: 2.45 GHz). Silica gel plates (Merck F_{254}) and silica gel 60 (Merck, 70-230 mesh) were used for analytical and column chromatography, respectively. All melting points were determined on a Gallenkamp melting point apparatus. Microanalyses were performed with a Perkin-Elmer 260 elemental analyzer for C, H, N and the results (reported in Table 2) were within ±0.4% of the theoretical values, unless stated otherwise. The IR spectra were recorded with a Perkin-Elmer Spectrum RX I spectrometer in Nujol mulls and are expressed in cm^{-1}. The 1H NMR spectra were obtained with a Brucker Avance 400 MHz instrument. The chemical shifts are reported in δ (ppm) and are relative to the central peak of the solvent which was DMSO-d_6 or $CDCl_3$. The following abbreviations are used: s = singlet, d = doublet, t = triplet, m = multiplet, br = broad, and ar = aromatic protons.

6.1.1. General procedure for the synthesis of 2-aryl-2,5-dihydro-4H-pyrazolo[3,4-*c*]quinolin-4-ones (28–31)

A suspension of suitable arylhydrazine hydrochlorides (9.2 mmol) and ethyl 2-(3-indolyl)-2-oxoethanoate[21] (4.6 mmol) in absolute ethanol (10 mL) and glacial acetic acid (5–6 drops) was microwave irradiated at 140 °C for 3 min (derivatives **28** and **29**), 130 °C for 10 min or 6 min (derivatives **30** and **31**, respectively). The suspension was cooled at room temperature and the solid collected, washed with water and re-crystallized.

Compound ***28***: yield 98%; mp > 300 °C (EtOH) (lit. mp > 300 °C).[14]

Compound ***29***: yield 50%; mp > 300 °C (AcOH) (lit. mp > 300 °C).[16]

Compound ***30***: yield 34%; mp > 300 °C (2-ethoxyethanol). ^{1}H NMR (DMSO-d_6) 7.26 (t, 1H, ar, *J* = 7.6 Hz), 7.36–7.41 (m, 2H, ar), 7.87–7.97(m, 3H, ar), 8.37–8.40 (m, 2H, ar), 9.66 (s, 1H, H-1), 11.54 (br s, lH, NH);IR 3146, 1689.

Compound ***31***: yield 36%; mp 279–281 °C (EtOH). ^{1}H NMR (DMSO-d_6) 2.26 (t, 1H, ar, *J* = 7.6 Hz), 7.38–7.41 (m, 2H, ar), 7.97 (d, 1H, ar, *J* = 7.7 Hz), 8.02 (d, 2H, ar, *J* = 8.6 Hz), 8.25 (d, 2H, ar, *J* = 8.6 Hz), 9.63 (s, 1H, H-l), 11.53 (br s, 1H, NH); IR 3150, 1669.

6.1.2. General procedure for the synthesis of 2-aryl-4-chloro-2H-pyrazolo[3,4-*c*]quinoline (32–35)

A mixture of **28–31** (3.6 mmol) and phosphorus pentachloride (1.1 mmol) in phosphorus oxychloride (20 mL) was heated at reflux for 2–3 h. Evaporation at reduced pressure of the excess of phosphorus oxychloride gave an oil which after treatment with cold water

Table 2
Combustion analysis data of the newly synthesized compounds

Compound	Formula	C Calcd-found	H Calcd-found	N Calcd-found
2	$C_{21}H_{14}N_4O_2$	71.18–71.30	3.98–3.71	15.81–15.65
3	$C_{21}H_{14}N_4O_2$	71.18–71.45	3.98–4.15	15.81–15.58
4	$C_22H_{16}N_4O_2$	71.73–71.58	4.38–4.12	15.21–15.44
5	$C_21H_{14}N_4OS$	68.09–68.24	3.81–3.69	15.12–15.35
6	$C_{21}H_{14}N_4OS$	68.09–68.19	3.81–4.02	15.12–14.95
7	$C_{20}H_{13}N_5OS$	64.68–64.41	3.53–3.86	18.86–19.08
8	$C_{22}H_{15}N_5O$	72.32–72.15	4.14–4.41	19.17–19.38
9	$C_{22}H_{15}N_5O$	72.32–72.55	4.14–4.33	19.17–19.01
10	$C_{22}H_{15}N_5O$	72.32–72.65	4.14–3.89	19.17–19.24
11	$C_{21}H_{14}N_6O$	68.84–68.60	3.85–4.08	22.94–22.75
12	$C_{21}H_{14}N_6O$	68.84–69.05	3.85–3.98	22.94–22.65
13	$C_{21}H_{14}N_6O$	68.84–68.99	3.85–3.44	22.94–23.11
14	$C_{22}H_{14}ClN_5O$	66.09–66.23	3.53–3.24	17.52–17.37
15	$C_{21}H_{13}ClN_4O_2$	64.87–64.51	3.37–3.02	14.41–14.29
16	$C_{24}H_{15}F_3N_4O$	66.66–66.90	3.50–3.28	12.96–12.72
17	$C_{24}H_{15}F_3N_4O$	66.66–66.73	3.50–3.87	12.96–12.68
18	$C_{24}H_{15}F_3N_4O$	66.66–66.80	3.50–3.76	12.96–13.06
19	$C_{24}H_{15}F_3N_4O$	66.66–66.46	3.50–3.19	12.96–13.15
20	$C_{24}H_{18}N_4O$	76.17–76.31	4.79–4.43	14.81–14.55
21	$C_{24}H_{18}N_4O$	76.17–76.39	4.79–5.00	14.81–14.51
22	$C_{32}H_{18}F_6N_4O_2$	63.58–63.70	3.00–2.86	9.27–9.41
23	$C_{32}H_{18}F_6N_4O_2$	63.58–63.33	3.00–3.28	9.27–9.03
26	$C_{17}H_nF_3N_4$	62.20–61.91	3.37–3.60	17.06–17.29
27	$C_{17}H_nF_3N_4$	62.20–61.98	3.37–3.01	17.06–17.14
30	$C_{17}H_{10}F_3N_3O$	62.01–62.22	3.06–3.28	12.76–12.50
31	$C_{17}H_{10}F_3N_3O$	62.01–62.31	3.06–2.94	12.76–12.92

(50 mL) yielded a solid which was quickly collected. The 4-chloro derivatives **32–35** were unstable, however they were pure enough to be characterized and used without further purification.

Compound ***32***: yield 90%, Ref. 16.

Compound ***33***: yield 84%, Ref. 16.

Compound ***34***: yield 85%; ^{1}H NMR (DMSO-d_6)7.71–7.76 (m, 2H, ar), 7.93–7.94 (m, 2H, ar), 8.01 (d, 1H, ar, *J* = 7.7 Hz), 8.30 (d, 1H, ar, *J* = 7.4 Hz), 8.47–8.48 (m, 2H, ar), 10.01 (s, 1H, H-1).

Compound ***35***: yield, 80%; ^{1}H NMR (DMSO-d_6) 7.71–7.75 (m, 2H, ar), 8.01 (d, 1H, ar, *J* = 7.9 Hz), 8.04 (d, 2H, ar, *J* = 8.4 Hz), 8.32 (d, 1H, ar, J = 7.9 Hz), 8.38 (d, 2H, ar, *J* = 8.4 Hz), 9.97 (s, 1H, H-1).

6.1.3. General procedure for the synthesis of 2-aryl-2H-pyrazolo[3,4-*c*]quinolin-4-amines (24–27)

A mixture of the suitable 4-chloro derivatives **32–35** (3 mmol) in absolute ethanol saturated with ammonia was heated overnight at 120 °C in a sealed tube. The solid that precipitated upon cooling was collected, washed with water and re-crystallized.

Compound ***24***: yield 85%; mp 198–199 °C (EtOAc) (lit. mp 197–198 °C).[16]

Compound ***25***: yield 65%; mp 244–246 °C (EtOH) (lit. mp 243–246 °C).[16]

Compound ***26***: yield 30%; mp 237–239 °C (EtOH); ^{1}H NMR (DMSO-d_6)7.06 (br s, 2H, NH_2), 7.26 (t, 1H, ar, *J* = 6.9 Hz), 7.42 (t, 1H, ar, *J* = 6.9 Hz), 7.51 (d, 1H, ar, *J* = 8.1 Hz), 7.86–7.90 (m, 2H, ar), 7.99 (d, 1H, ar, *J* = 7.7 Hz), 8.45 (d, 1H, ar, *J* = 8.2 Hz), 8.51 (s, 1H, ar), 9.67 (s, 1H, H-1); IR 3465, 3306, 1653.

Compound ***27***: yield 45%; mp 272–275 °C (EtOH); ^{1}H NMR (DMSO-d_6)7.12 (br s, 2H, NH_2), 7.26 (t, 1H, ar, *J* = 6.9 Hz), 7.41 (t, 1H, ar, *J* = 6.9 Hz), 7.53 (d, 1H, ar, *J* = 7.8 Hz), 8.00 (d, 1H, ar, *J* = 7.8 Hz), 8.02 (d, 2H, ar, *J* = 8.4 Hz), 8.35 (d, 2H, ar, *J* = 8.4 Hz), 9.65 (s, 1H, H-1); IR 3460, 3295, 1648.

6.1.4. General procedures for the synthesis of 2-aryl-2H-pyrazolo[3,4-*c*]quinolin-4-amides (2–21)

The title compounds **2–21** were synthesized following the same procedure but employing different stoichiometric ratios among the starting amino derivatives **24**–**27** and the reagents (Methods A–C).

6.1.4.1. Method A (compounds 2, 5, 7–10, 20, 21). A mixture of the 4-amino derivative **24** (1 mmol), the suitable carboxylic acid (7 mmol), 1-(3-(dimethylamino)propyl)-3-ethyl-carbodiimide hydrochloride (7 mmol), 1-hydroxybenzotriazole (7 mmol), triethylamine (15 mmol) and 4-(dimethylamino)pyridine (0.1 mmol) in anhydrous dimethylformamide (2–3 mL) was stirred at room temperature until the disappearance of the starting 4-amino derivative (TLC monitoring, 3–85 h). The solid was filtered off and the cooled (0 °C) mother liquor was diluted with water (about 15–20 mL). The precipitated solid was collected and re-crystallized from the suitable solvent.

Compound ***2***: yield 90%; mp 193–194 °C (EtOH); ^{1}H NMR ($CDCl_3$) 6.59–6.60 (m, 1H, furane H-4 proton), 7.41–7.66 (m, 8H, 6ar + 2 furane protons), 7.95 (d, 1H, ar, *J* = 7.7 Hz), 8.02 (d, 2H, ar, *J* = 7.8 Hz), 8.70 (s, 1H, H-1); IR 3389, 1703.

Compound ***5***: yield 70%; mp 188–189 °C (2-methoxyethanol); ^{1}H NMR ($CDCl_3$) 7.17–7.18 (m, 1H, thiophene proton), 7.43–7.62 (m, 7H, 6 ar + 1 thiophene proton), 7.95 (d, 1H, ar, *J* = 7.6 Hz), 8.02 (d, 2H, ar, *J* = 8.0 Hz), 8.12–8.13 (m, 1H, thiophene proton), 8.71 (s, 1H, H-1).

Compound ***7***: yield 85%; mp 215–217 °C (EtOAc/EtOH); ^{1}H NMR (DMSO-d_6) 7.53–7.71 (m, 5H, ar), 7.92 (d, 1H, ar, *J* = 7.2 Hz), 8.13 (d, 2H, ar, *J* = 8.0 Hz), 8.26 (d, 1H, ar, *J* = 6.7 Hz), 8.68 (s, 1H, thiazole proton), 9.39 (s, 1H, thiazole proton), 9.75 (s, 1H, H-1), 10.73 (s, 1H, NH); IR 3358, 1702.

Compound ***8***: yield 82%; mp 220–222 °C (2-methoxyethanol); ^{1}H NMR (DMSO-d_6)7.53–7.71 (m, 5H, ar), 7.78–7.81 (m, 1H, ar), 7.93 (d, 1H, ar, *J* = 7.4 Hz), 8.13–8.30 (m, 5H, ar), 8.86 (d, 1H, pyridine proton, *J* = 4.4 Hz), 9.75 (s, 1H, H-1), 11.33 (s, 1H, NH); IR 3324, 1711.

Compound ***9***: yield 50%; mp 231–233°C (2-methoxyethanol); ^{1}H NMR ($CDCl_3$) 7.28–7.64 (m, 7H, ar), 7.99–8.00 (d, 1H, ar, *J* = 7.8 Hz), 8.05 (d, 2H, ar, *J* = 8.0 Hz), 8.74–8.78 (m, 3H, 2 ar + H-1), 9.68 (br s, 1H, ar).

Compound ***10***: yield 80%; mp 246–248 °C (2-methoxyethanol); ^{1}H NMR ($CDCl_3$) 7.50–7.63 (m, 6H, ar), 8.00–8.06 (m, 3H, ar), 8.32–8.33 (m, 2H, ar), 8.76 (s, 1H, H-1), 8.82–8.83 (m, 2H, ar).

Compound ***20***: yield 40%; mp 170–172 °C (EtOH); ^{1}H NMR ($CDCl_3$) 2.50 (s, 3H, Me), 7.38–7.78 (m, 8H, ar), 7.95–8.05 (m, 3H, ar), 8.21–8.29 (m, 2H, ar), 8.77 (s, 1H, H-1).

Compound ***21***: yield 50%; mp 115–116 °C (cyclohexane/EtOAc); ^{1}H NMR ($CDCl_3$) 2.47 (s, 3H, Me), 7.44 (d, 2H, ar, *J* = 7.9 Hz), 7.45–7.68 (m, 6H, ar), 7.98 (d, 1H, ar, *J* = 7.7 Hz), 8.03 (d, 2H, ar, *J* = 7.9 Hz), 8.34 (d, 2H, ar, *J* = 7.7 Hz), 8.74 (s, 1H, H-1).

6.1.4.2. Method B (compounds 3, 4, 6, 11–13). The 4-amino derivative **24** (1 mmol) was reacted with the commercially available 3-furyl- (5 mmol), 3-thienyl- (6 mmol), 2-pyrazinyl- (3 mmol) carboxylic acids, and with the synthesized 2-(5-methylfuryl)-2-pyrimidyl- and 4-pyrimidyl-carboxylic acids (4 mmol) in the presence of 1-(3-(dimethylamino)propyl)-3-ethyl-carbodiimide hydrochloride (3 mmol), 1-hydroxybenzotriazole (3 mmol), triethylamine (5 mmol) and 4-(dimethylamino)pyridine (0.1 mmol) in anhydrous dimethylformamide (2–3 mL). The reaction mixture was stirred at room temperature until the disappearance of the starting 4-amino derivative (TLC monitoring, 50–160 h). The insoluble solid was filtered off and the cooled (0 °C) dimethylformamide solution diluted with water (about 10–20 mL) to yield a precipitate which was collected and re-crystallized from suitable solvent. For compound **13**, the reaction mixture was filtered and the solid washed with water and re-crystallized.

Compound ***3***: yield 55%; mp 127–130 °C (EtOH); ^{1}H NMR ($CDCl_3$) 7.03 (s, 1H, furane proton), 7.44–7.59 (m, 7H, ar), 7.96 (d, 1H, ar, *J* = 7.8 Hz), 8.02 (d, 2H, ar, *J* = 8.2 Hz), 8.46 (s, 1H, furane proton), 8.76 (s, 1H, H-1); IR 3300–3550, 1625.

Compound ***4***: yield 60%; mp 167–169 °C (EtOH); ^{1}H NMR ($CDCl_3$) 2.48 (s, 3H, Me), 6.21 (d, 1H, furane proton, *J* = 3.3 Hz), 7.45–7.61 (m, 7H, 5ar + 2 furane protons), 7.97 (d, 1H, ar, *J* = 7.7 Hz), 8.02 (d, 2H, ar, J = 7.9 Hz), 8.74 (s, 1H, H-9), IR 1624.

Compound ***6***: yield 65%; mp 147–150 °C (EtOH); ^{1}H NMR ($CDCl_3$) 7.35–7.37(m, 1H, thiophene proton), 7.44–7.62 (m, 6H, ar), 7.85 (d, 1H, thiophene proton, *J* = 5.0 Hz), 7.96 (d, 1H, ar, *J* = 7.7 Hz), 8.01 (d, 2H, ar, *J* = 8.1 Hz), 8.52 (d, 1H, thiophene proton, *J* = 3.0 Hz), 8.72 (s, 1H, H-1); IR 3550, 3490, 1630.

Compound ***11***: yield 40%; mp 168–172 °C (2-methoxyethanol); ^{1}H NMR (DMSO-d_6)7.53–7.85 (m, 7H, ar), 8.14 (d, 2H, ar, *J* = 7.9 Hz), 8.23 (d, 1H, ar, *J* = 8.1 Hz), 9.10 (d, 2H, pyrimidine protons, *J* = 4.7 Hz), 9.74 (s, 1H, H-1), 11.32 (br s, 1H, NH); IR 3474, 3337, 1720.

Compound ***12***: yield 45%; mp 195–198 °C (2-ethoxyethanol); ^{1}H NMR (DMSO-d_6)7.55 (t, 1H, ar, *J* = 7.1 Hz), 7.64–7.71 (m, 4H, ar), 7.93–8.26 (m, 5H, ar), 9.23 (d, 1H, pyrimidine proton, *J* = 4.6 Hz), 8.54 (s, 1H, ar), 9.77 (s, 1H, ar), 11.26 (br s, 1H, NH); IR 3425, 3315, 1707.

Compound ***13***: yield 87%; mp 249–251 °C (2-ethoxyethanol); ^{1}H NMR (DMSO-d_6)7.56 (t, 1H, ar, *J* = 7.3 Hz), 7.64–7.71 (m, 4H, ar), 7.95 (d, 1H, ar, *J* = 7.7 Hz), 8.13 (d, 2H, ar, *J* = 7.9 Hz), 8.26 (d, 1H, *J* = 7.0 Hz), 8.93 (s, 1H, ar), 9.03 (s, 1H, ar), 9.40 (s, 1H, ar), 9.76 (s, 1H, ar), 11.12 (br s, 1H, NH);IR3395, 1716.

6.1.4.3. Method C (compounds 14–19). A mixture of the 4-amino derivatives **24–27** (1 mmol), the suitable carboxylic acid (3 mmol), 1-(3-(dimethylamino)propyl)-3-ethyl-carbodiimide hydrochloride (3 mmol), 1-hydroxybenzotriazole (3 mmol), triethylamine (5 mmol) and 4-(dimethylamino)pyridine (0.1 mmol) in anhydrous dimethylformamide (2–3 mL) was stirred at room temperature until the disappearance of the starting amino derivative (TLC monitoring, 6–140 h). For compound **14**, the reaction mixture was filtered and the solid was washed with water and purified by column chromatography (eluent CHCl3/MeOH, 9:1). For compounds **15, 16–19**, the reaction mixture was diluted with ice water (about 10–20 mL) to yield a solid which was collected by filtration and washed with water. Crude compounds **15, 16**, **18**, 19 were purified by re-crystallization from suitable solvent while compound **17** was purified by column chromatography (eluent CH_2Cl_2/EtOAc, 9:1).

Compound ***14***: yield 25%; mp 192–194 °C (EtOH); ^{1}H NMR ($CDCl_3$) 7.53 (t, 1H, ar, *J* = 8.2 Hz), 7.60–7.61 (m, 4H, ar) 8.01–8.03 (m, 3H, ar), 8.43–8.44 (m, 2H, ar), 8.71 (s, 1H, H-1), 8.85 (d, 2H, pyridine protons, *J* = 5.0 Hz); IR 3200–3500, 1625.

Compound ***15***: yield 15%; mp 251–252 °C (EtOH/2-methoxyethanol); ^{1}H NMR ($CDCl_3$) 6.60–6.61 (m, 1H, furane proton), 7.47 (t, 1H, ar, *J* = 7.9 Hz), 7.62–7.67 (m, 6H, 4ar + 2 furane protons), 7.96–8.01 (m, 3H, ar), 8.71 (s, 1H, H-1); IR 3300–3500, 1708.

Compound ***16***: yield 89%; mp 211–213 °C (2-methoxyethanol); ^{1}H NMR (DMSO-d_6) 7.56–7.67 (m, 5H, ar), 7.89–7.90 (m, 3H, ar), 8.10–8.22 (m, 3H, ar), 8.43–8.45 (m, 2H, ar), 9.89 (s, 1H, H-9), 11.10 (br s, 1H, NH); IR 3233, 1646.

Compound ***17***: yield 63%; mp 201–202 °C (MeOH); ^{1}H NMR (DMSO-d_6)7.56–7.67 (m, 5H, ar), 7.90–7.92 (m, 1H, ar), 8.04 (d, 2H, ar, *J* = 8.4 Hz), 8.19–8.23 (m, 3H, ar), 8.33 (d, 2H, ar, *J* = 8.4 Hz), 9.88 (s, 1H, H-l), 11.11 (br s, 1H, NH).

Compound ***18***: yield 60%; mp 188–190 °C (EtOH); ^{1}H NMR ($CDCl_3$) 7.46–7.62 (m, 7H, ar), 7.81 (d, 1H, ar, *J* = 7.4 Hz), 7.98 (d, 1H, ar, *J* = 7.6 Hz), 8.05 (d, 2H, ar, *J* = 7.7 Hz), 8.71–8.75 (m, 3H, ar).

Compound ***19***: yield 74%; mp 204–207 °C (EtOH); ^{1}H NMR ($CDCl_3$) 7.47–7.64 (m, 6H, ar), 7.77 (d, 2H, ar, *J* = 7.8 Hz), 7.98 (d, 1H, ar, *J* = 7.8 Hz), 8.04 (d, 2H, ar, *J* = 8.7 Hz), 8.61 (d, 2H, ar, *J* = 7.8 Hz), 8.73 (s, 1H, H-1).

6.1.5. General procedure for the synthesis of 2-phenyl-4-[bis(3-trifluoromethylbenzoyl)]amino-pyrazolo[3,4-*c*]quinoline (22) and 2-phenyl-4-[bis(4-trifluoromethylbenzoyl)]amino-pyrazolo[3,4-*c*]quinoline (23)

The title compounds **22** and **23** were obtained by refluxing the 4-amino derivative **24** (2 mmol) with an excess (5.0 mmol) of 3-trifluoromethylbenzoyl chloride and 4-trifluoromethylbenzoyl chloride, respectively, in anhydrous methylene chloride (5 mL) and pyridine (5.0 mmol). The suspension was refluxed until the disappearance of the starting material (TLC monitoring, 24–48 h), then cooled at room temperature. The solid was collected by filtration, washed with water and re-crystallized.

Compound ***22***: yield 45%; mp 213–214 °C (EtOH); ^{1}H NMR (DMSO-d_6) 7.53 (t, 1 H, ar, *J* = 7.1 Hz), 7.61–7.74 (m, 6H, ar), 7.82 (d, 1H, ar, *J* = 7.9 Hz), 7.94 (d, 2H, ar, J = 7.6 Hz), 8.03 (d, 2H, ar, *J* = 7.8 Hz), 8.15–8.19 (m, 4H, ar), 8.31 (d, 1 H, ar, *J* = 8.0 Hz), 9.81 (s, 1H, H-9); IR 1726, 1690.

Compound ***23***: yield 35%; mp 252–254 °C (2-methoxyethanol/EtOH); ^{1}H NMR (DMSO-d_6) 7.53 (t, 1H, ar, *J* = 7.2 Hz), 7.61–7.72 (m, 5H, ar), 7.79 (d, 4H, ar, *J* = 8.0 Hz), 8.03 (d, 2H, ar, *J* = 7.8 Hz), 8.09 (d, 4H, ar, *J* = 8.1 Hz), 8.31 (d, 1H, ar, *J* = 7.8 Hz), 9.85 (s, 1H, H-9); IR 1730, 1700.

6.2. Molecular modeling studies

6.2.1. Computational methodologies

All molecular modeling studies were performed on a 2 CPU (PIV 2.0–3.0 GHZ) Linux PC. Homology modeling and docking studies were carried out using Molecular Operating Environment (MOE, version 2007.09) suite.[26] All ligand structures were optimized using RHF/AM1 semiempirical calculations, and the software package MOPAC implemented in MOE was utilized for these calculations.[29]

6.2.2. Homology model of the human A_3 receptor

A homology model of the human A_3 receptor was built using the X-ray crystal structure of the resting state bovine rhodopsin (pdb code: 1L9H;[30] available at the RCSB Protein Data Bank, http://www.rcsb.org) with a 2.6-Å resolution as template. The amino acid sequences of TM helices of the human A_3 receptor and bovine rhodopsin were aligned, and in this phase some GPCRs highly conserved amino acid residues worked as guide, including the DRY motif (D3.49, R3.50, Y3.51, or D107, R108, Y109, respectively) and three Pro residues (P4.60, P6.50, P7.50 or P145, P189, P245, respectively). The boundaries identified from the X-ray crystal structure of bovine rhodopsin were applied for the corresponding sequences of the TM helices of the A_3 receptor. The loop domains of the human A_3 receptor were built by the *loop search method* implemented in MOE. Special care had to be given to the second extracellular (E2) loop, which folds back over TM domains. This loop limits the dimension of the active site, and its amino acids could be involved in direct interactions with the ligands. The presence of a conserved disulfide bridge between cysteines in TM3 and E2 might be the driving force to this particular fold of the E2 domain, so this loop was modeled using a rhodopsin-like constrained geometry around the E2-TM3 disulfide link. Because of the limited sequence similarity between the human A_3 receptors and the template in the C-terminal domain, only a short segment of this region was modeled. In particular, the model ends with the Ser306 residue corresponding to the Asp330 residue of the bovine rhodopsin template. Once the heavy atoms were modeled, all hydrogen atoms were added, and the protein coordinates were then minimized with MOE using the AMBER99 force field.[31] The minimizations were performed by 1000 steps of steepest descent followed by conjugate gradient minimization until the RMS gradient of the potential energy was less than 0.05 kJ mol^{-1} $Å^{-1}$.

6.2.3. TM binding site identification and refining

The human A_3 receptor binding site region was established with the aid of published site directed mutagenesis data, which indicated in particular that residues His95, Ser247, Asn250, and His272 are important for ligand binding.[25] As this receptor region did not contain a suitable cavity for antagonist docking, a manual docking section was performed in which compound 1 was inserted in the established binding site assuming a number of different orientations. Thus, an equivalent number of protein–ligand complexes was obtained. Each complex was then minimized. In this step, the coordinates of a sphere of residues in proximity of ligand structure (6 Å) were left unfixed, while the remaining receptor residue coordinates were fixed.

The unfixed atom sets were the same for all different receptor–ligand complexes. Even in this case, the minimizations were performed by 1000 steps of steepest descent followed by conjugate gradient minimization until the RMS gradient of the potential energy was less than 0.05 kJ mol^{1} Å^{1}. The final step was the measurement of potential energy of the different receptor conformations (extracted from the respective receptor–ligand complexes) with the MOE potential energy tool. The receptor conformation with the lowest potential energy value was selected for the following docking section.

6.2.4. Molecular docking of the human A_3 receptor antagonists

All antagonist structures were docked into the refined TM binding site by using the MOE Dock tool. This method is divided into a number of stages: Conformational analysis of ligands. The algorithm generated conformations from a single 3D conformation by conducting a systematic search. In this way, all combinations of angles were created for each ligand. *Placement*. A collection of poses was generated from the pool of ligand conformations using Alpha Triangle placement method. Poses were generated by superposition of ligand atom triplets and triplets of points in the receptor binding site. The receptor site points are alpha sphere centers which represent locations of tight packing. At each iteration a random conformation was selected, a random triplet of ligand atoms and a random triplet of alpha sphere centers were used to determine the pose. *Scoring*. Poses generated by the placement methodology were scored using two available methods implemented in MOE, the London dG scoring function which estimates the free energy of binding of the ligand from a given pose, and Affinity dG Scoring which estimates the enthalpic contribution to the free energy of binding. The top 30 poses for each ligand were output in a MOE database. Each resulting ligand pose was then subjected to MMFF94[32–38] energy minimization until the RMS gradient of the potential energy was less than 0.05 kJ mol^{-1} Å^{-1}. In this phase, AMBER99 partial charges of receptor and MOPAC output partial charges of ligands were conserved. The minimized docking conformations were then re-scored using both London dG scoring function and Affinity dG scoring method.

6.2.5. Pharmacophore model

The pharmacophore model was developed from docking conformations using the Pharmacophore Query Editor tool implemented in MOE. In particular, Pharmacophore Consensus tool created a list of suggested features from the superimposed docking conformations, based on specified consensus parameters. Suggested features were converted to query features and were considered to develop the pharmacophore model.

6.2.6. Molecular descriptors and druggability evaluation

A set of molecular descriptors were calculated for compounds **1**–**23**, **26**, **27**, **30**, **31**, **36**–**38** with MOE software. The descriptors, taken from MOE software documentation, are as follows. log*S*: log of the aqueous solubility (mol/L); this property is calculated from an atom contribution linear atom type model[39] with $r^2 = 0.90$, ~1, 200 molecules. log*P* (o/w): log of the octanol/water partition coefficient (including implicit hydrogen atoms); this property is calculated from a linear atom type model with $r^2 = 0.931$, RMSE = 0.393 on ~1, 827 molecules; Weight: molecular weight (including implicit hydrogen atoms) in atomic mass units with atomic weights; a_acc: number of hydrogen bond acceptor atoms (not counting acidic atoms but counting atoms that are both hydrogen bond donors and acceptors such as –OH); **a_don:** number of hydrogen bond donor atoms (not counting basic atoms but counting atoms that are both hydrogen bond donors and acceptors such as -OH); ASA: water accessible surface area calculated using a radius of 1.4 Å for the water molecule. A polyhedral representation is used for each atom in calculating the surface area; h: number of heavy atoms; VSA: van der Waals surface area. A polyhedral representation is used for each atom in calculating the surface area; **ASA_H:** water accessible surface area of all hydrophobic ($|_qi| < 0.2$) atoms; **ASA_P:** water accessible surface area of all polar ($|q_i| > = 0.2$) atoms. The **lip_violation** parameter indicates the number of violations of Lipinski's 'rule of five';[40] the **drug-like** parameter is the estimation of molecular druggability, and it is indicated as '*y*' if and only if lip_violation parameter = 0, otherwise '*n*'. The values of the molecular descriptors and the other calculated parameters are reported in the Supplementary data.

6.3. Pharmacological assays

6.3.1. Human cloned A1, A_{2A}, and A_3 adenosine receptor binding assay

All synthesized compounds were tested to evaluate their affinity at human A1, A_{2A} and A_3 adenosine receptors. Displacement experiments of [^{3}H]DPCPX (1 nM) to hA_1 CHO membranes (50 μg of protein/assay) and at least six to eight different concentrations of antagonists for 120 min at 25 °C in 50 mM Tris–HCl buffer pH 7.4 were performed.[41] Non-specific binding was determined in the presence of 10 μM of CHA (<10% of the total binding). Binding of [^{3}H]ZM-241385 (1 nM) to hA_{2A}CHO membranes (50 μg of protein/assay) was performed using 50 mM Tris–HCl buffer, 10 mM $MgCl_2$ pH 7.4 and at least six to eight different concentrations of antagonists studied for an incubation time of 60 min at 4 °C.[42] Non-specific binding was determined in the presence of 1 μM ZM-241385 and was about 20% of total binding. Competition binding experiments to hA_3 CHO membranes (50 μg of protein/assay) and 0.5 nM [^{125}I]AB-MECA, 50 mM Tris–HCl buffer, 10 mM $MgCl_2$, 1 mM EDTA, pH 7.4 and at least six to eight different concentrations of examined ligands for 120 min at 4°C.[43] Non-specific binding was defined as binding in the presence of 1 μM AB-MECA and was about 20% of total binding. Bound and free radioactivity were separated by filtering the assay mixture through Whatman GF/B glass fiber filters using a Brandel cell harvester. The filter bound radioactivity was counted by Scintillation Counter Packard Tri Carb 2500 TR with an efficiency of 58%.

6.3.2. Rat A_3 adenosine receptor binding assays

Selected compounds were tested for evaluating their affinity at rat A_3 adenosine receptors expressed in HEK 293 cells (Perkin-Elmer, Boston, USA). Competition binding experiments to rA_3 HEK membranes (10 μg of protein/assay) and 0.5 nM [^{125}I]AB-MECA, 50 mM Tris–HCl buffer, 10 mM $MgCl_2$, 1 mM EDTA, pH 7.4 and at least 3–4 different concentrations of examined ligands for 120 min at 25 °C.[43] Non-specific binding was defined as binding in the presence of 1 μM AB-MECA and was about 20% of total binding. Bound and free radioactivity were separated by filtering the assay mixture through Whatman GF/B glass fiber filters by using a Brandel cell harvester. The filter bound radioactivity was counted by Scintillation Counter Packard Tri Carb 2500 TR with an efficiency of 58%.

6.3.3. Measurement of cyclic AMP levels in CHO cells transfected with hA_2B or hA_3 adenosine receptors

CHO cells transfected with hAR subtypes were washed with phosphate-buffered saline, diluted tripsine and centrifuged for 10 min at 200*g*. The pellet containing the CHO cells (1×10^6 cells/assay) was suspended in 0.5 ml of incubation mixture (mM): NaCl 15, KCl 0.27, NaH_2PO4 0.037, $MgSO_4$ 0.1, $CaCl_2$ 0.1, Hepes 0.01, $MgCl_2$ 1, glucose 0.5, pH 7.4 at 37 °C, 2 IU/ml adenosine deaminase and4-(3-butoxy-4-methoxybenzyl)-2-imidazolidinone (Ro 20–1724) as phosphodiesterase inhibitor and preincubated for 10 min in a shaking bath at 37 °C. The potency of antagonists to A_{2B} receptors was determined by antagonism of NECA (200 nM)-induced stimulation of cyclic AMP levels. In addition, the potency of antagonists to A_3 receptors was determined in the presence of forskolin 1 μM and Cl-IB-MECA (100 nM) that mediated inhibition of cyclic AMP levels. The reaction was terminated by the addition of cold 6% trichloroacetic acid (TCA). The TCA suspension was centrifuged at 2000*g* for 10 min at 4 °C and the supernatant was extracted four times with water saturated diethyl ether. The final aqueous solution was tested for cyclic AMP levels by a competition protein binding assay. Samples of cyclic AMP standard (0–10 pmol) were added to each test tube containing [^{3}H] cyclic AMP and the incubation buffer (trizma base 0.1 M, aminophylline 8.0 mM, 2-mercaptoethanol 6.0 mM, pH 7.4). The binding protein prepared from beef adrenals, was added to the samples previously incubated at 4 °C for 150 min, and after the addition of charcoal were centrifuged at 2000*g* for 10 min. The clear supernatant was counted in a Scintillation Counter Packard Tri Carb 2500 TR with an efficiency of 58%.[44]

6.3.4. Data analysis

The protein concentration was determined according to a Bio-Rad method[45] with bovine albumin as a standard reference. Inhibitory binding constant, K_i, values were calculated from those of IC_{50} according to Cheng and Prusoff equation $K_i = IC_50/(1+[C^*]/K_D^*)$, where $[C^*]$ is the concentration of the radioligand and K_D^* its dissociation constant.[46] A weighted non-linear least-squares curve fitting program LIGAND[47] was used for computer analysis of inhibition experiments. EC_{50} and IC_{50} values obtained in cyclic AMP assay were calculated by non-linear regression analysis using the equation for a sigmoid concentration–response curve (GraphPAD Prism, San Diego, CA, USA).

Acknowledgment

The work was supported by a grant from the Italian Ministry for University and Research (MIUR, FIRB RBNE03YA$_3$L project).

Supplementary data

Supplementary data associated with this article can be found, in the online version, at doi:10.1016/j.bmc.2008.10.018.

References and notes

1. Jacobson, K. A.; Knutsen, L. J. S.. In *Handbook of Experimental Pharmacology: Purinergic and Pyrimidinergic Signalling I*; Abbracchio, M. P., Williams, M., Eds.; Springer: Berlin, 2001; Vol. 151, p 129.
2. Fredholm, B. B.; Ijzerman, A. P.; Jacobson, K. A.; Klotz, K. N.; Linden, J. *Pharmacol. Rev.* **2001**, *53*, 527.
3. Abbracchio, M. P.; Brambilla, R.; Ceruti, S.; Kim, H. O.; von Lubitz, D. K.; Jacobson, K. A.; Cattabeni, F. *Mol. Pharmacol.* **1995**, *48*, 1038.
4. Ali, H.; Choi, O. H.; Fraundorfer, P. F.; Yamada, K.; Gonzaga, H. M.; Beaven, M. A. *J. Pharmacol. Exp. Ther.* **1996**, *276*, 837.
5. Shneyvays, V.; Leshem, D.; Zinman, T.; Mamedova, L. K.; Jacobson, K. A.; Shainberg, A. *Am. J. Physiol. Heart Circ. Physiol.* **2005**, *288*, H2792.
6. Schulte, G.; Fredholm, B. B. *Cell Signal.* **2003**, *15*, 813.
7. Brambilla, R.; Cattabeni, F.; Ceruti, S.; Barbieri, D.; Franceschi, C.; Kim, Y. C.; Jacobson, K. A.; Klotz, K. N.; Lohse, M. J.; Abbracchio, M. P. *Naunyn-Schmiedeberg's Arch. Pharmacol.* **2000**, *361*, 225.
8. Merighi, S.; Mirandola, P.; Varani, K.; Gessi, S.; Leung, E.; Baraldi, P. G.; Tabrizi, M. A.; Borea, P. A. *Pharmacol. Ther.* **2003**, *100*, 48.
9. Merighi, S.; Benini, A.; Mirandola, P.; Gessi, S.; Varani, K.; Leung, E.; Maclennan, S.; Borea, P. A. *Biochem. Pharmacol.* **2006**, *72*, 19.
10. Lee, H. T.; Ota-Setlik, A.; Xu, H.; D'Agati, V. D.; Jacobson, M. A.; Emala, C. W. *Am. J. Physiol. Renal Physiol.* **2003**, *284*, F267.
11. Yang, H.; Avila, M. Y.; Peterson-Yantorno, K.; Coca-Prados, M.; Stone, R. A.; Jacobson, K. A.; Civan, M. M. *Curr. Eye Res.* **2005**, *30*, 747.
12. Pugliese, A. M.; Coppi, E.; Spalluto, G.; Corradetti, R.; Pedata, F. *Br. J. Pharmacol.* **2006**, *147*, 524.
13. Pugliese, A. M.; Coppi, E.; Volpini, R.; Cristalli, G.; Corradetti, R.; Jeong, L. S.; Jacobson, K. A.; Pedata, F. *Biochem. Pharmacol.* **2007**, *74*, 768.
14. Colotta, V.; Catarzi, D.; Varano, F.; Capelli, F.; Lenzi, O.; Filacchioni, G.; Martini, C.; Trincavelli, L.; Ciampi, O.; Pugliese, A. M.; Pedata, F.; Schiesaro, A.; Morizzo, E.; Moro, S. J. *Med. Chem.* **2007**, *50*, 4061.
15. Colotta, V.; Catarzi, D.; Varano, F.; Cecchi, L.; Filacchioni, G.; Martini, C.; Trincavelli, L.; Lucacchini, A. J. *Med. Chem.* **2000**, *43*, 1158.
16. Colotta, V.; Catarzi, D.; Varano, F.; Cecchi, L.; Filacchioni, G.; Martini, C.; Trincavelli, L.; Lucacchini, A. J. *Med. Chem.* **2000**, *43*, 3118.
17. Colotta, V.; Catarzi, D.; Varano, F.; Calabri, F. R.; Lenzi, O.; Filacchioni, G.; Martini, C.; Trincavelli, L.; Deflorian, F.; Moro, S. J. *Med. Chem.* **2004**, *47*, 3580.
18. Catarzi, D.; Colotta, V.; Varano, F.; Lenzi, O.; Filacchioni, G.; Trincavelli, L.; Martini, C.; Montopoli, C.; Moro, S. *Med. Chem.* **2005**, *48*, 7932.
19. Lenzi, O.; Colotta, V.; Catarzi, D.; Varano, F.; Filacchioni, G.; Martini, C.; Trincavelli, L.; Ciampi, O.; Varani, K.; Marighetti, F.; Morizzo, E.; Moro, S. J. *Med. Chem.* **2006**, *49*, 3916.
20. Morizzo, E.; Capelli, F.; Lenzi, O.; Catarzi, D.; Varano, F.; Filacchioni, G.; Vincenzi, F.; Varani, K.; Borea, P. Andrea; Colotta, V.; Moro, S. J. *Med. Chem.* **2007**, *50*, 6596.
21. Casnati, G.; Ricca, A. *Gazz. Chim. Ital.* **1963**, *93*, 355.
22. Robert, J. M. H.; Robert-Piessard, S.; Courant, J.; Le Baut, G.; Robert, B.; Lang, F.; Petit, J. Y.; Grimaud, N.; Welin, L. *Eur. J. Med. Chem.* **1995**, *30*, 915.
23. Dunn, G. E.; Lawler, E. A.; Yamashita, A. B. *Can. J. Chem.* **1977**, *55*, 2478.
24. Tagawa, Y.; Yamashita, K.; Higuchi, Y.; Goto, Y. *Heterocycles* **2003**, *60*, 953.
25. Moro, S.; Spalluto, G.; Jacobson, K. A. *Trends Pharmacol. Sci.* **2005**, *26*, 44.
26. Molecular Operating Environment (MOE 2007.09); C.C.G., Inc., 1255 University St., Suite 1600, Montreal, Quebec, Canada H3B 3X3.
27. Tafi, A.; Bernardini, C.; Botta, M.; Corelli, F.; Andreini, M.; Martinelli, A.; Ortore, G.; Baraldi, P. G.; Fruttarolo, F.; Borea, P. A.; Tuccinardi, T. J. *Med. Chem.* **2006**, *49*, 4085.
28. Moro, S.; Braiuca, P.; Deflorian, F.; Ferrari, C.; Pastorin, G.; Cacciari, B.; Baraldi, P. G.; Varani, K.; Borea, P. A.; Spalluto, G. J. *Med. Chem.* **2005**, *48*, 152.
29. Stewart, J. J. *J. Comput. Aided Mol. Des.* **1990**, *4*, 1.
30. Okada, T.; Fujiyoshi, Y.; Silow, M.; Navarro, J.; Landau, E. M.; Shichida, Y. *Proc. Natl. Acad. Sci. U.S.A.* **2002**, *99*, 5982.
31. Cornell, W. D.; Cieplak, P.; Bayly, C. I.; Gould, I. R.; Merz, K. M.; Ferguson, D. M.; Spellmeyer, D. C.; Fox, T.; Caldwell, J. W.; Kollman, P. A. *Am. Chem. Soc.* **1995**, *117*, 5179.
32. Halgren, T. A. J. *Comput. Chem.* **1996**, *17*, 490.
33. Halgren, T. A. J. *Comput. Chem.* **1996**, *17*, 520.
34. Halgren, T. A. J. *Comput. Chem.* **1996**, *17*, 553.
35. Halgren, T. A. J. *Comput. Chem.* **1996**, *17*, 587.
36. Halgren, T. A.; Nachbar, R. J. *Comput. Chem.* **1996**, *17*, 616.
37. Halgren, T. A. J. *Comput. Chem.* **1999**, *20*, 720.
38. Halgren, T. A. J. *Comput. Chem.* **1999**, *20*, 730.
39. Hou, T. J.; Xia, K.; Zhang, W.; Xu, X. J. J. *Chem. Inf. Comput. Sci.* **2004**, *44*, 266.
40. Lipinski, C. A.; Lombardo, F.; Dominy, B. W.; Feeney, P. J. *Adv. Drug Deliv. Rev.* **1997**, *23*, 3.
41. Borea, P. A.; Dalpiaz, A.; Varani, K.; Gessi, S.; Gilli, G. *Life Sci.* **1996**, *59*, 1373.
42. Varani, K.; Rigamonti, D.; Sipione, S.; Camurri, A.; Borea, P. A.; Cattabeni, F.; Abbracchio, M. P.; Cattaneo, E. *FASEB J.* **2001**, *15*, 1245.
43. Varani, K.; Cacciari, B.; Baraldi, P. G.; Dionisotti, S.; Ongini, E.; Borea, P. A. *Life Sci.* **1998**, *63*, 81.
44. Varani, K.; Gessi, S.; Merighi, S.; Vincenzi, F.; Cattabriga, E.; Benini, A.; Klotz, K. N.; Baraldi, P. G.; Tabrizi, M. A.; Lennan, S. M.; Leung, E.; Borea, P. A. *Biochem. Pharmacol.* **2005**, *70*, 1601.
45. Bradford, M. M. *Anal. Biochem.* **1976**, *72*, 248.
46. Cheng, Y.; Prusoff, W. H. *Biochem. Pharmacol.* **1973**, *22*, 3099.
47. Munson, P. J.; Rodbard, D. *Anal. Biochem.* **1980**, *107*, 220.